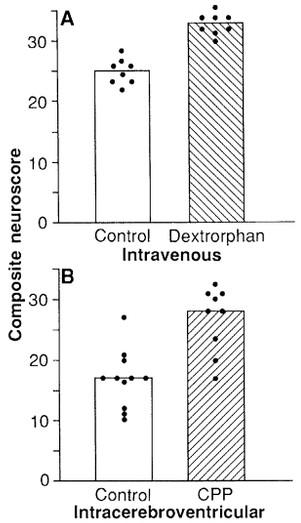

Fig. 3. (**A**) The effects of treatment with intravenous dextrorphan or an equal volume of physiological saline on behavioral outcome 2 weeks after moderate fluid percussion injury. Composite neurological scores reflect the summation of seven functional scores (each rated 0 to 5). Dextrorphan-treated animals showed significantly improved behavioral recovery after trauma as compared to controls (Mann-Whitney U test, $P < 0.01$). These are the same animals that were evaluated by MRS as shown in Fig. 2. Dots represent individual animal scores, and histograms represent median values. (**B**) Effects of treatment with the competitive NMDA antagonist CPP or an equal volume of vehicle (artificial CSF), administered by intracerebroventricular injection before injury, on behavioral outcome after severe (2.85 atm) fluid percussion–induced TBI. Rats treated with CPP showed significantly better behavioral recovery 2 weeks after trauma than controls (Mann-Whitney U test, $P < 0.005$).

Our studies demonstrate that levels of EAAs increase in the extracellular space after CNS trauma and that NMDA antagonists have beneficial effects in TBI, as reflected by metabolic and behavioral markers of injury. Taken together, our data indicate that TBI is associated with the release of EAAs, which contribute to neurological dysfunction after trauma through actions at NMDA receptors. Treatment with a noncompetitive NMDA antagonist improved the cellular bioenergetic state in the acute period after trauma and limited neurological dysfunction. Beneficial behavioral effects were also found with a competitive NMDA antagonist.

The mechanisms by which EAAs contribute to secondary tissue injury remain speculative, although increases in intracellular Na^+ and Ca^{2+} have been implicated in this delayed injury process (*16*). However, TBI causes a marked decrease in intracellular free Mg^{2+} as well as a decline in total tissue Mg^{2+}, the amount of which is correlated with injury severity (*11, 14*). Dextrorphan treatment reversed the decrease in Mg_f found after trauma, which is consistent with recent findings showing that treatment with the noncompetitive NMDA antagonist MK-801 partially restores total tissue Mg^{2+} levels after traumatic spinal cord injury (*17*). The ability of NMDA antagonists to restore Mg^{2+} levels after injury may be related to the improvement in cellular bioenergetic state observed after dextrorphan treatment and may, in part, underlie the protective effects of NMDA antagonists in brain trauma.

REFERENCES AND NOTES

1. R. P. Simon, J. H. Swan, T. Griffiths, B. S. Meldrum, *Science* **226**, 850 (1984).
2. T. Wieloch, *ibid.* **230**, 681 (1985).
3. B. K. Siesjo and T. Wieloch, *Central Nervous System Trauma Status Report* (National Institute of Neurological and Communicative Disorders and Stroke Publication) (Byrd, Richmond, 1985), p. 260; A. I. Faden, *Clin. Neuropharmacol.* **10**, 193 (1987).
4. J. W. Olney *et al.*, *Neurosci. Lett.* **68**, 29 (1986).
5. D. Lodge, N. A. Anis, N. R. Burton, *ibid.* **29**, 281 (1982); J. Davies and J. C. Watkins, *Exp. Brain Res.* **49**, 280 (1983).
6. R. Vink, T. K. McIntosh, M. W. Weiner, A. I. Faden, *J. Cereb. Blood Flow Metab.* **7**, 563 (1987).
7. R. Vink, T. K. McIntosh, I. Yamakami, A. I. Faden, *Magn. Reson. Med.* **6**, 37 (1988).
8. V. Ungerstedt, in *Measurement of Neurotransmitter Release in Vivo*, G. A. Marsden, Ed. (Wiley, Chichester, England, 1984), pp. 81–105.
9. S. Cortez, T. K. McIntosh, L. Noble, *Brain Res.* **482**, 271 (1989).
10. P. Demediuk, M. P. Daly, A. I. Faden, *Trans. Am. Soc. Neurochem.* **19**, 214 (1988); *J. Neurochem.*, in press.
11. R. Vink, T. K. McIntosh, P. Demediuk, M. Weiner, A. I. Faden, *J. Biol. Chem.* **15**, 757 (1988).
12. C. P. George, M. P. Goldberg, D. W. Choi, G. K. Steinberg, *Brain Res.* **440**, 375 (1988).
13. B. Chance, S. Eleff, J. S. Leigh, *Proc. Natl. Acad. Sci. U.S.A.* **77**, 7430 (1980).
14. R. Vink, T. K. McIntosh, P. Demediuk, A. I. Faden, *Biochem. Biophys. Res. Commun.* **149**, 594 (1987).
15. D. E. Murphy, J. Schneider, C. Boehm, J. Lehmann, M. Williams, *J. Pharmacol. Exp. Ther.* **240**, 778 (1987).
16. D. W. Choi, *J. Neurosci.* **7**, 369 (1987).
17. A. I. Faden, M. Lemke, R. P. Simon, L. J. Noble, *J. Neurotrauma* **5**, 33 (1988).

18. Supported, in part, by a grant from the Centers for Disease Control to A.I.F. R.V. is a recipient of a Queen Elizabeth II fellowship. We thank R. Romhanyi and V. A. Head for technical assistance and C. Warri and E. Leveau for preparation of the manuscript. We thank D. Choi for providing dextrorphan and for helpful suggestions in reviewing the report.

20 December 1988; accepted 17 March 1989

Regulation of Calcium Release Is Gated by Calcium Current, Not Gating Charge, in Cardiac Myocytes

MICHAEL NÄBAUER, GEERT CALLEWAERT, LARS CLEEMANN, MARTIN MORAD*

In skeletal muscle, intramembrane charge movement initiates the processes that lead to the release of calcium from the sarcoplasmic reticulum. In cardiac muscle, in contrast, the similarity of the voltage dependence of developed tension and intracellular calcium transients to that of calcium current suggests that the calcium current may gate the release of calcium. Nevertheless, a mechanism similar to that of skeletal muscle continues to be postulated for cardiac muscle. By using rapid exchange (20 to 50 milliseconds) of the extracellular solutions in rat ventricular myocytes in which the intracellular calcium transients or cell shortening were measured, it has now been shown that the influx of calcium through the calcium channel is a mandatory link in the processes that couple membrane depolarization to the release of calcium. Thus, intramembrane charge movement does not contribute to the release of calcium in heart muscle.

THE EXCITATION-CONTRACTION COUPLING mechanisms may be qualitatively different in skeletal and cardiac muscle (*1*). In skeletal muscle, the signal for the release of calcium is associated with charge movement at the junction between the transverse tubule (T) and the sarcoplasmic reticulum (SR). Thus, the intramembrane charge movement (*2*), the intracellular Ca^{2+} transient (*3*), the development of tension (*4*), and the intrinsic birefringence signal associated with Ca^{2+} release (*5*) all show sigmoid voltage dependence. By contrast, in mammalian myocardium, the voltage dependence of intracellular Ca^{2+} transients (*6*), development of tension (*7*) and cell shortening (*8*), and the intrinsic birefringence signal (*9*) are bell-shaped and reflect the voltage dependence of the Ca^{2+} current (i_{Ca}) rather than the voltage dependence of the charge movement (*10*). Furthermore, Ca^{2+} may be released by repolarization from positive potentials (*6*), a finding inconsistent with release triggered by intramembrane charge movement. Recently, however, Cannell *et al.* (*11*) suggested that the release of Ca^{2+} from the intracellular pools in rat ventricular myocytes may be in part regulated by a charge-coupled release mechanism.

University of Pennsylvania, Department of Physiology, Philadelphia, PA 19104.

*To whom correspondence should be addressed.

Here we show that it is exclusively Ca^{2+} influx through the Ca^{2+} channel rather than intramembrane charge movement that regulates Ca^{2+} release in cardiac myocytes.

Rat ventricular myocytes were enzymatically isolated (*12*) and were voltage-clamped with the whole-cell patch-clamp technique (*13*). Cells were dialyzed with 100 m*M* CsCl, 5 m*M* magnesium adenosine triphosphate, 0.02 to 0.1 m*M* adenosine 3′,5′-monophosphate (cAMP), 20 m*M* tetraethylammonium chloride, and 20 m*M* Hepes, *p*H 7.2. Intracellular Ca^{2+} was partially buffered either with small concentrations of BAPTA [1,2 bis-(*o*-aminophenoxy) ethane-*N*,*N*,*N*′,*N*′-tetraacetic acid] (50 to 100 μ*M*) in experiments where cell shortening was measured or with fura-2 (200 to 400 μ*M*) in experiments where the intracellular Ca^{2+} activity was measured. Addition of BAPTA or fura-2 to the dialysate increased the buffering capacity of the myocytes. However, Ca^{2+} signals were not significantly affected since we saw uniform values of Ca^{2+} transients (500 to 800 n*M*) when buffer concentrations varied from 50 to 400 μ*M*. In addition, Ca^{2+} release induced by caffeine caused significant Ca^{2+} extrusion current via the Na^+-Ca^{2+} exchanger (see for instance, Figs. 1A and 2).

The control external solution contained 140 m*M* NaCl, 5.4 m*M* KCl or 10 m*M* CsCl, 2 or 3 m*M* $CaCl_2$, 0.02 m*M* tetrodotoxin, 10 m*M* glucose, 10 m*M* Hepes-NaOH, *p*H 7.4 at room temperature (21 to 23°C). Cell shortening was monitored with a 256-element linear photodiode array (*14*). Intracellular Ca^{2+} transients were measured with fura-2 and a dual wavelength excitation system (*15*). External solutions were exchanged rapidly (20 to 50 ms) around the voltage-clamped cells with a multibarreled pipette with a common opening large enough to prevent turbulence of flow (*16*). The measurements of intracellular Ca^{2+} transients and of cell shortening were performed in two parallel series of experiments. Each record of the intracellular Ca^{2+} activity is representative of experiments with three to five cells. Recordings of cell shortening are representative of experiments with five to eight cells.

We examined the effect of rapid removal of Ca^{2+} from the bathing solution in rat ventricular myocytes and measured the intracellular Ca^{2+} transients or cell contraction. Voltage-clamp pulses were applied from −60 mV to 0 mV at 5-s intervals, and current through the Ca^{2+} channel and intracellular Ca^{2+} transients were measured simultaneously (Fig. 1A). In the presence of Ca^{2+}, depolarizing pulses to 0 mV evoked a Ca^{2+} current that was accompanied by intracellular Ca^{2+} release (*6*) (Fig. 1A, left panel). Exchanging the external solution for one containing no added Ca^{2+} and 4 m*M* EGTA 500 ms before the next depolarizing pulse induced a large and slowly inactivating Na^+ current through the Ca^{2+} channel (Fig. 1A, middle panel). Amplitude and time course of the Na^+ current through the Ca^{2+} channel reached their final values in the first clamp pulse, indicating that the exchange of the external solution was complete in less than 500 ms. Nevertheless, the large influx of Na^+ through the Ca^{2+} channel failed to activate intracellular Ca^{2+} release. A short application of 5 m*M* caffeine was used to check whether the intracellular Ca^{2+} stores were still intact during exposure to 4 m*M* EGTA. Addition of caffeine in 0 Ca^{2+} solution containing 4 m*M* EGTA induced a large intracellular Ca^{2+} transient, which in turn activated a transient inward current, reflecting the extrusion of Ca^{2+} by the Na^+-Ca^{2+} exchanger (*17*) (Fig. 1A, right panel).

Similar conclusions were reached in experiments where cell shortening was measured (Fig. 1B). In the absence of external

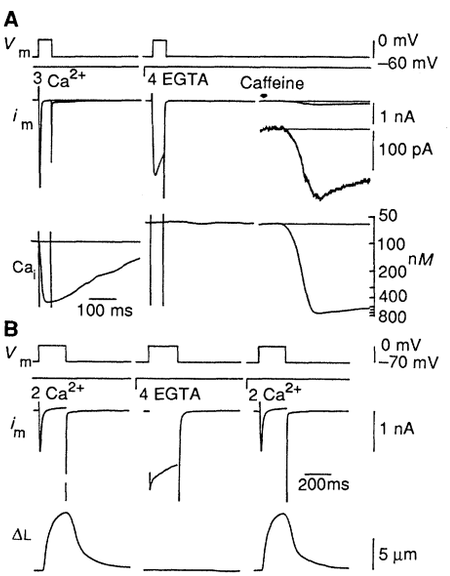

Fig. 1. Na^+ current through the Ca^{2+} channel does not activate Ca^{2+} release in rat ventricular myocytes. (**A**) Intracellular Ca^{2+} transients (Ca_i) and membrane currents (i_m) in a myocyte loaded with fura-2 and superfused with 3 m*M* Ca^{2+}. The intracellular Ca^{2+} signal is the fluorescence signal measured with excitation at 410 nm but calibrated in terms of the intracellular Ca^{2+} concentration. The calibration of the Ca^{2+} signal in this panel and in Fig. 2 show Ca^{2+} transients that are typical of ratio measurements (335-nm and 410-nm excitation) in 11 cells. (Left panel) Control conditions, 3 m*M* Ca^{2+}; (middle panel) 4 m*M* EGTA; (right panel) 5 m*M* caffeine. (**B**) Cell shortening (ΔL) and membrane current (i_m) measured during three subsequent depolarizations from −70 mV to 0 mV. (Left panel) Control records, 2 m*M* external Ca^{2+}; (middle panel) 4 m*M* EGTA and no added Ca^{2+}; (right panel) control conditions, 2 m*M* Ca^{2+}.

Ca^{2+}, the influx of Na^+ through the Ca^{2+} channel was unable to induce cell shortening (Fig. 1B, middle panel). Because a selective depletion of the physiologically significant Ca^{2+} pools by EGTA might not be detected by the use of caffeine, the integrity of the intracellular Ca^{2+} stores was tested by reexposure of the myocytes to solutions containing normal external Ca^{2+} concentrations. Calcium current and cell contraction recovered immediately to control levels (Fig. 1B, right panel). Thus, in the presence of 4 m*M* EGTA, the intracellular Ca^{2+} stores are intact and the influx of Na^+ through the Ca^{2+} channel is unable to gate the release of Ca^{2+} from the SR.

These experiments were performed under conditions where most of the activator Ca^{2+} is released from the SR. This assertion is based on the findings that the i_{Ca} is insufficient to account for the measured intracellular Ca^{2+} transients; that ryanodine, which blocks release of Ca^{2+} from the SR, blocks 80 to 90% of the intracellular Ca^{2+} transients (*6*); and that several beats are required to reestablish normal intracellular Ca^{2+} transients or contractions once the intracellular stores have been depleted by repeated caffeine exposures (see Fig. 3B). The absence of depolarization-induced Ca^{2+} transients and contraction in the middle panels of Fig. 1 therefore indicate that when there is no influx of Ca^{2+} through the surface membrane, there is also no release of Ca^{2+} from the SR.

We also tested the effect of the absence of significant Ca^{2+} influx through the Ca^{2+} channel by omitting external Ca^{2+} (Fig. 2). In such solutions, the contaminant Ca^{2+} concentrations (5 to 15 μ*M* as measured with a Ca^{2+}-selective electrode) were sufficient to effectively block Na^+ influx through the Ca^{2+} channel (*18, 19*). Both i_{Ca} and intracellular Ca^{2+} transients were eliminated within one beat (Fig. 2, middle panel). Once again, application of caffeine (5 m*M*) in nominally Ca^{2+}-free solution induced a large release of Ca^{2+} and activated a transient inward current, consistent with the assertion that intracellular Ca^{2+} pools remained intact during the withdrawal of Ca^{2+} (see also Fig. 1).

In skeletal muscle, all of the cations of group IA and IIA of the periodic table (including Na^+, K^+, Mg^{2+}, Ca^{2+}, and Ba^{2+}) support intramembrane charge movement in the T-SR junction (*20*), a finding consistent with observations that contractions are retained in Ca^{2+}-free solutions in skeletal muscle (*21*). In rat cardiac myocytes, the suppression of the Ca^{2+} current by omission of external Ca^{2+} or the activation of a large Na^+ influx through the Ca^{2+} channel in the presence of 4 m*M* EGTA

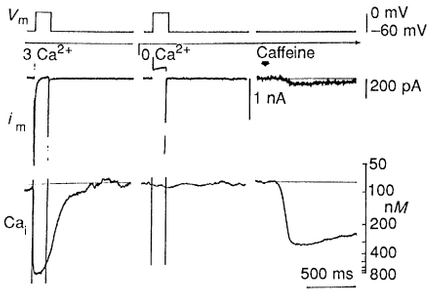

Fig. 2. Ca^{2+} release requires significant flow of Ca^{2+} current through the Ca^{2+} channel. (Left panel) Membrane current (i_m) and intracellular Ca^{2+} transient (Ca_i) in 3 m*M* external Ca^{2+}. No significant Ca^{2+} current was flowing through the Ca^{2+} channel and Ca^{2+} release was not activated on depolarization (middle panel). Extracellular solution nominally Ca^{2+}-free (Ca^{2+} contamination, 5 to 15 μ*M*). (Right panel) 5 m*M* caffeine.

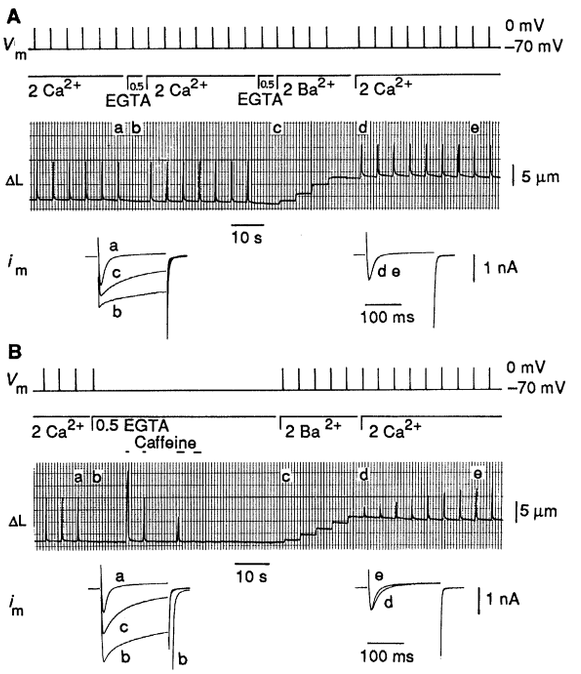

Fig. 3. Effectiveness of Ba^{2+} as a substitute for Ca^{2+} in releasing Ca^{2+} from the sarcoplasmic reticulum. (**A**) Chart recording of cell shortening (ΔL) of a myocyte superfused with the solutions indicated above it. The uppermost trace is the voltage-clamp protocol (V_m); clamp duration was 200 ms at 5-s intervals. The lower traces are the corresponding current (i_m), as marked in the chart recording; a, 2 m*M* external Ca^{2+}; b, 0.5 m*M* EGTA and no added Ca^{2+}; c, the first depolarizing pulse in 2 m*M* Ba^{2+}; d and e, 2 m*M* Ca^{2+}. (**B**) Effect of intracellular Ca^{2+} depletion on cell shortening in Ba^{2+}. Chart recording of cell shortening (ΔL) with the respective membrane currents (i_m) given in the lower traces. a, 2 m*M* external Ca^{2+}; b, 0.5 m*M* EGTA and no added Ca^{2+}. The cell was then superfused four times with 5 m*M* caffeine twice for 40 ms, then twice for 1000 ms. c, 2 m*M* Ba^{2+}; d and e, 2 m*M* external Ca^{2+}.

does not support excitation-contraction coupling, even though the ionic constituents were appropriate to support charge movement (*20*). Thus, Ca^{2+} release from cardiac SR is not regulated by intramembrane charge movement associated with depolarization or gating of the Ca^{2+} channel (Figs. 1 and 2).

Because Ba^{2+} is effectively transported by the Ca^{2+} channel (*18*) and also supports intramembrane charge movement related to excitation-contraction coupling in skeletal muscle (*20*), we tested whether Ba^{2+} could replace Ca^{2+} as the activator of Ca^{2+} release in cardiac myocytes. Depolarizing pulses (200-ms duration) from −70 to 0 mV were applied at 5-s intervals and cell shortening and current through the Ca^{2+} channel were measured simultaneously (Fig. 3). To ensure Ca^{2+} removal from the extracellular space, exposure to Ba^{2+} was preceded by superfusion of the cell with 0.5 m*M* EGTA for 5 s. Depolarizing pulses in Ba^{2+} solution caused Ba^{2+} influx through the Ca^{2+} channel (Fig. 3A, trace c), which led to maintained and stepwise decreases in cell length. In the presence of Ba^{2+}, no significant relaxation was observed between the depolarizing steps. On re-exposure to Ca^{2+}, regular contractions immediately resumed with an amplitude similar to control values before exposure to Ba^{2+}, even though the baseline cell length was significantly decreased (Fig. 3A). This result suggests that the Ca^{2+} stores were not released by the influx of Ba^{2+} and that the stepwise cell shortening in Ba^{2+} was the result of a direct effect of Ba^{2+} on the myofilaments. The Ba^{2+}-induced decrease in baseline cell length subsided very slowly over 5 to 6 min after re-exposure to Ca^{2+}-containing solutions.

To rule out the possibility that the cell shortening during depolarizing pulses in Ba^{2+}-containing solutions was caused by slow release of Ca^{2+} from the SR, the intracellular Ca^{2+} stores were first depleted by short, repetitive applications of 5 m*M* caffeine in 0.5 m*M* EGTA-containing solutions. In the presence of Ba^{2+}, depolarizing pulses still induced stepwise cell shortening similar to that observed in myocytes not pretreated with caffeine (compare Fig. 3B with Fig. 3A). Thus, the stepwise cell shortening is probably related to the direct interaction of Ba^{2+} with the myofilaments (*22*). In myocytes where the SR was depleted of Ca^{2+}, i_{Ca} recovered immediately upon re-exposure to Ca^{2+}-containing solutions, but six to eight beats were required for full restoration of contraction (Fig. 3B), consistent with the recirculation hypothesis (*1*). In such a scheme, a fraction of the released Ca^{2+} is resequestered by the SR as the remaining Ca^{2+} is extruded across the sarcolemma. Thus, although Ba^{2+} substitutes effectively for Ca^{2+} as a charge carrier through the Ca^{2+} channel, it fails to gate the release of Ca^{2+}, suggesting the specificity of the release mechanism for Ca^{2+}.

In cells dialyzed with fura-2 where extracellular Ca^{2+} was replaced by Ba^{2+}, these results were confirmed. That is, Ba^{2+} markedly suppressed the rate and magnitude of the fura-2 fluorescence signal. The rate of relaxation of the fluorescence signal was also extremely slow, resulting in stepwise increases in baseline fluorescence, quite similar to the pattern observed when cell length was measured (Fig. 3). Upon application of caffeine, a large change in fluorescence was observed that was accompanied by a transient inward current, suggesting that the content of Ca^{2+} pools was intact. Consistent with the findings of Fig. 3, in vitro studies showed a strong affinity of Ba^{2+} for fura-2 (*23*), indicating that the observed fluorescence change was due to direct binding of Ba^{2+} to fura-2 and not to the release of Ca^{2+} from the SR. This idea was also supported by calculations showing that the Ba^{2+} current through the Ca^{2+} channel carries sufficient Ba^{2+} into the cell to produce the observed changes in fluorescence or cell shortening (*22, 24*) (Fig. 3).

Our results indicate that Ca^{2+} entry through the Ca^{2+} channel is required to trigger the release of Ca^{2+} from the SR. The absence of significant Ca^{2+} current or the influx of Na^+ or Ba^{2+} through the Ca^{2+} channel do not support depolarization-induced release. However, the removal of Ca^{2+} might inactivate charge movement by shifting its inactivation to more negative potentials. We do not think this is the case because in skeletal muscle, in the absence of external Ca^{2+}, the inactivation of Ca^{2+} release shifts to more negative potentials by 29 mV (*25*); although most of our experiments were carried out at holding potentials of −60 to −80 mV, in several experiments with holding potentials as negative as −100 mV, we did not find a qualitative change in the results.

Rapid (20 to 50 ms) exchange of extracellular solutions allows for removal of extracellular Ca^{2+} without significantly altering the Ca^{2+} content of the SR. Our results show the Ca^{2+} requirement of the Ca^{2+} release process and are consistent with the Ca^{2+}-induced Ca^{2+} release hypothesis (*26*). The results do not support a contribution of a charge-coupled mechanism to the release of Ca^{2+} in cardiac myocytes.

REFERENCES AND NOTES

1. M. Morad and Y. Goldman, *Prog. Biophys. Mol. Biol.* **27**, 257 (1973).
2. W. Melzer, M. F. Schneider, B. J. Simon, G. Szucs, *J. Physiol. (London)* **373**, 481 (1986).
3. G. Brum, E. Stefani, E. Rios, *Can. J. Physiol. Pharmacol.* **65**, 681 (1987).
4. A. L. Hodgkin and P. Horowicz, *J. Physiol. (London)* **153**, 386 (1960); P. Heistracher and C. C. Hunt, *ibid.* **201**, 589 (1969); C. Caputo and P. Fernandez de Bolanos, *ibid.* **289**, 175 (1979).
5. L. Kovacs and M. F. Schneider, *Nature* **265**, 556 (1977); S. Baylor and W. K. Chandler, in *Biophysical Aspects of Cardiac Muscle*, M. Morad, Ed. (Academic Press, New York, 1978), pp. 207–228.
6. G. Callewaert, L. Cleemann, M. Morad, *Proc. Natl. Acad. Sci. U.S.A.* **85**, 2009 (1988).
7. G. W. Beeler, Jr., and H. Reuter, *J. Physiol. (London)* **207**, 211 (1970).
8. B. London and J. W. Krueger, *J. Gen. Physiol.* **88**, 475 (1986).
9. J. Maylie and M. Morad, *J. Physiol. (London)* **357**, 267 (1984).
10. B. P. Bean and E. Rios, *Biophys. J.* **53**, 158a (1988).
11. M. B. Cannell, J. R. Berlin, W. J. Lederer, *Science* **238**, 1419 (1987).
12. R. Mitra and M. Morad, *Am. J. Physiol.* **249**, H1056 (1985).
13. O. P. Hamill, A. Marty, E. Neher, B. Sakmann, F. J. Sigworth, *Pfluegers Arch.* **395**, 6 (1981).
14. Myocyte shortening was measured by projecting the image of the cell edge on a linear 256-element photodiode array. The position of the cell edge was determined at 4-ms intervals and converted into absolute changes in cell length. The output signal was filtered at 500 Hz.
15. For measurement of intracellular Ca^{2+} transients, cells were loaded with fura-2 (pentapotassium salt) via the pipette. A mirror oscillating at 1.2 kHz was used as a mechanical light chopper for dual wavelength excitation at 330 and 410 nm. Fluorescence emission was measured at 510 nm. Details are given in (*6*).
16. A. Konnerth, H. D. Lux, M. Morad, *J. Physiol. (London)* **386**, 603 (1987).
17. S. Mechmann and L. Pott, *Nature* **319**, 597 (1986).
18. P. Hess and R. W. Tsien, *ibid.* **309**, 453 (1984).
19. W. Almers, E. W. McCleskey, P. T. Palade, *J. Physiol. (London)* **353**, 565 (1984).
20. G. Pizarro, R. Fitts, E. Rios, *Biophys. J.* **53**, 645a (1988).
21. C. M. Armstrong, F. M. Bezanilla, P. Horowicz, *Biochim. Biophys. Acta* **267**, 605 (1972).
22. Y. Saeki, C. Kato, T. Horikoshi, K. Yanagisawa, *Pfluegers Arch.* **400**, 235 (1984).
23. Spectrophotometric measurements with 0.4 m*M* fura-2 in a 0.5-mm cuvette showed that the Ba^{2+}-induced change in the absorption spectrum is nearly identical to that induced by Ca^{2+} and the binding constant for Ba^{2+} is less than 50 μM.
24. A 2-nA Ba^{2+} current flowing for the duration of a 200-ms clamp pulse will add 2 fmol [2 nA × 0.2/(2 × Faraday constant)] to an intracellular volume of 20 pl (10 μm × 20 μm × 100 μm), thereby changing the total intracellular Ba^{2+} concentration by 2 fmol/20 pl or 100 μM. Thus Ba^{2+} will bind to a significant fraction of the troponin C and fura-2 molecules.
25. G. Brum, E. Rios, E. Stefani, *J. Physiol. (London)* **398**, 441 (1988).
26. A. Fabiato, *J. Gen. Physiol.* **85**, 189, 247 and 291 (1985).
27. Supported by NIH grants R01-HL16152 and R01-HL33720. M.N. was supported by the Deutsche Forschungsgemeinschaft.

14 November 1988; accepted 1 March 1989

Induction of Mesoderm by a Viral Oncogene in Early *Xenopus* Embryos

MALCOLM WHITMAN AND D. A. MELTON

During frog embryogenesis, mesoderm is specified in the equatorial region of the early embryo by a signal from the vegetal hemisphere. Prospective ectodermal cells dissected from the animal hemisphere can be respecified to form mesodermal tissues by recombination with vegetal tissue or by treatment with any of several polypeptide growth factors or growth factor–like molecules. Together with the discovery that several developmental mutations in *Drosophila* are in genes with significant homology to mammalian mitogens and oncogenes, these observations suggest that early developmental signals may use similar transduction pathways to mitogenic signals characterized in cultured mammalian cells. Whether mesoderm can be induced by activation of intracellular signal transduction pathways implicated in mitogenesis and oncogenesis has been investigated with the viral oncogene polyoma middle T. Microinjection of middle T messenger RNA into early embryos results in the respecification of isolated prospective ectodermal tissue to form characteristic mesodermal structures. Middle T in frog blastomeres appears to associate with cellular activities similar to those observed in polyoma-transformed mouse cells, and transformation-defective middle T mutants fail to induce mesoderm. These results suggest that early inductive signals and mitogenic and oncogenic stimuli may share common signal transduction pathways.

INTERCELLULAR SIGNALS ARE IMPORTANT in establishing the fundamental body plan and controlling the formation of organ systems during embryogenesis. These signals mediate early tissue-tissue interactions, called embryonic inductions, which have been well defined in amphibians by explantation and transplantation of embryonic tissues (*1, 2*). The earliest of these interactions is the induction of mesoderm by an interaction between presumptive endodermal and ectodermal tissues. Mesoderm normally forms from cells at the junction between the animal and vegetal hemispheres of the embryo (the marginal zone). Explanted cells from the animal hemisphere (animal caps) form only ectodermal tissue when cultured in isolation, but these same cells will form mesodermal tissue when placed in contact with vegetal (endodermal) cells (*1*). Several polypeptide growth factors or growth factor–like molecules [fibroblast growth factor (FGF), transforming growth factor–β2 (TGF-β2), and XTC mesoderm-inducing factor (MIF)] have been identified that can mimic the action of vegetal tissue in the induction of mesoderm in animal caps (*3–6*). Although the role of these growth factor–like molecules in the natural inductive process has not yet been directly demonstrated, maternal transcripts encoding FGF and a TGF-β homologous peptide (Vg1) have been identified in early embryos (*5, 7*). These observations suggest that membrane-associated signal transduction mechanisms associated with the mitogenic action of growth factors such as FGF may also be involved in early embryonic induction.

Although pharmacological agents are available for the investigation of a few signal transduction pathways in *Xenopus* embryos, for example, 12-*O*-tetradecanoyl phorbol-13-acetate (TPA) as an exogenous activator of protein kinase C (*8*), microinjection of

Table 1. Induction of mesoderm by middle T mRNA injection. Summary of mesoderm induction in isolated animal caps by microinjected middle T mRNA as distinguished by morphological elongation and histological identification of muscle and notochord.

Affected area	Control (H_2O)	Mutant middle T (NG59)	Wild-type middle T
Elongation/constriction	3/144 (2%)	11/152 (7%)	57/142 (40%)
Notochord	0/25 (0%)	0/35 (0%)	10/62 (16%)
Muscle	0/30% (0%)	0/39% (0%)	17/55 (31%)

Department of Biochemistry and Molecular Biology, Harvard University, 7 Divinity Avenue, Cambridge MA 02138.